A Petrophysical Model to Distinguish Water-Wet and Oil-Wet Fractions of Unconventional Reservoir Systems Using Triple-Combo Log Suites*

Michael Holmes[1], Antony Holmes[1], and Dominic I. Holmes[1]

[1]Digital Formation, Inc., Denver, CO (Michael.Holmes@DigitalFormation.com)

Abstract

Measurements of fluid wetting characteristic are made routinely on rock samples. However, there are no published petrophysical models to differentiate between oil-wet and water-wet fractions of a reservoir sequence using commonly available log suites. This presentation builds on our previous publication that describes the unconventional reservoir petrophysical model we have developed (Holmes, 2014). Essentially, we define four porosity components, namely total organic carbon, clay porosity, effective porosity, and "free shale porosity." This last component is an indirect calculation if the first three components do not sum to total porosity.

Porosity/resistivity plots can be constructed for the total porosity and interpreted in a standard fashion. These will mostly indicate a water-wet system where the effective porosity fraction is examined. A second porosity/resistivity plot compares resistivity with "free shale porosity," and is clearly interpreted to indicate Archie saturation exponents of much larger than 2 - frequently in excess of 3 - indicating the oil-wet fraction of the reservoir system. Additionally, the plots suggest low to very low values of cementation exponent, ranging from 1.0 to 1.5.

Examples from the Bakken of Montana and North Dakota, the Niobrara of Colorado, and the Wolfcamp and Spraberry of Texas are presented showing quantitative distinction of water-wet vs. oil-wet reservoir components.

Introduction

It is commonly recognized that mixed wetting occurs in unconventional oil reservoir systems - part of the porosity fabric is water-wet and part is oil-wet. Measurements are made on rock samples to define wetting characteristics. However, in addition, there are data available from triple-combo log suites which can be analyzed to define wetting characteristics.

For conventional reservoir petrophysical analysis the model shown in Figure 1 is used.

Holmes (2014) presented an unconventional reservoir petrophysical model and defined four porosity components (Figure 2):

• Total organic carbon (TOC)
• Clay mineral porosity
• Standard effective porosity
• Free shale porosity

In addition to examining the influence of clay fluids, it is necessary to define the contribution of the other components on log responses.

This article addresses the analysis of the shale components using deterministic approaches involving triple-combo log suites. Particular emphasis is directed to differentiating electrical responses of the clean formation and shale.

The goal is to calculate the four porosity components (Figure 2 and Figure 3):

• Effective Porosity (Phi_E) - clay-free porosity in the non-shale fraction.
• Clay Porosity (Phi_{Clay}).
• Free Shale Porosity (Phi_{FS}) - newly-defined porosity component is usually a small volume (mostly less than 5% of the total rock volume) and is believed to contain free hydrocarbons and perhaps also formation water.
• Total Organic Carbon (TOC) - a combination of kerogen and bitumen and contains adsorbed hydrocarbons.

Free shale porosity is interpreted to be secondary porosity associated with TOC, generated during the thermal maturation process of organic material.

Glorioso, et al. (2012) published examples of secondary porosity derived from SEM images (Figure 4 and Figure 5).

The model published by Glorioso (Figure 6) is similar to the model presented here:

The emphasis of this article is to examine resistivity responses of the effective porosity fraction as compared with those of the free shale porosity fraction. Free shale porosity is equivalent to free gas in kerogen pores (Figure 6).

Procedures to Identify the Four Porosity Components in Unconventional Reservoirs

The following analytic procedures are used:

1. A standard shaley formation analysis is performed to quantify:
    a. Shale Volume – VSH

b. Total porosity – PhiT
c. Effective porosity – PhiE
d. Fluid components in effective porosity
e. Matrix volume and petrophysical responses – Vma

A density/neutron combination to calculate porosity is preferred (Figure 7), as this is essentially not affected by changing matrix density and fluid content (gas vs. oil and water)

2. Total organic content (TOC) is calculated using two techniques:

a. The Passey, et al. (1990) ΔlogR technique (Figure 8) is used to differentiate between organic rich and organic lean shales. The calculation of TOC (in weight percent) can be made for any available porosity log. Input of the level of organic metamorphism (LOM) or vitrinite reflectance (Ro), a

b. Schmoker (1989) relates TOC to density response, recognizing TOC has a significantly lower density than most of the other reservoir components.

For both methods it is necessary to convert TOC in weight percent to volume percent. TOC density ranges from about 1.1 g/cc to 1.8 g/cc, and is probably a function of thermal maturity. Choice of the correct density is important since the range is so large.

3. From the standard density/neutron measurements, all non-shale components together (with TOC volume calculations) are subtracted to yield a shale-only density/neutron comparison (Figure 9). This provides an estimate of clay mineral species.

The non-shale components are:

a. Effective porosity – accounting for fluid content
b. Matrix volume – accounting for rock lithology
c. Total organic carbon as a volume fraction

All non-shale components are calculated on a 100% rock volume using individual values of shale volume. Clay porosity is calculated as the product of cross plot porosity and VSH.

4. Free shale porosity is calculated by subtracting the other porosity components from total porosity:

Free Shale Porosity = Effective Porosity - Clay Porosity

Clearly, free shale porosity is zero or greater. If negative values are calculated it might be a consequence of incorrect estimates of shale volume and TOC volume and/or an incorrect assumption of TOC weight percent. Additionally, there may be an incorrect weight to volume conversion for TOC. A depth plot of free shale porosity will help in the interpretation – data cannot fall in the pink shaded region (Figure 10).

Influence of Reservoir Wetting on Archie Parameters

Archie (1942) presented an empirical equation to determine water saturation:

$$S_W{}^n = \frac{aR_W}{Phi_T^m \times R_t}$$

Where:

S_W = water saturation
a = empirical factor, usually assumed to be 1.0
R_W = water resistivity
R_t = formation resistivity
m = cementation exponent, a rock property, often assumed to be 2.0
n = saturation exponent, a fluid property, often assumed to be equal to m

As wettability to oil increases, 'n' also increases (Keller, 1953; Sweeney and Jennings, 1960; Ransom, 1995).

Graphical interpretation of log porosity vs. log resistivity cross plots (Pickett, 1966) can be used to interpret m, n, and R_W. Alignment of data not residing on the 100% S_W line can be used to estimate n. Buckles (1965) derived a relationship between effective porosity, Phi_E, and irreducible water saturation, S_{Wi}.

$$Phi_E \times S_{Wi} = constant$$

$Phi_E \times S_{Wi}$ is the bulk volume of irreducible or immobile water.

The magnitude of the constant (mostly between 2% and 10%) is dependent on rock lithology and rock fabric. Holmes (2009) suggested that the Buckles relation is a specific solution to a more general relation:

$$Phi_E^Q \times S_{Wi} = constant$$

The exponent Q is frequently 1.0 (original Buckles), but can range from about 0.8 to 1.6.

Linear alignment of data on the Pickett plot away from the S_W=100% line is indicative of rocks belonging to a singular value of $Phi_E \times S_{Wi}$. The slope of the alignment is a function of n. If the data show a negative slope then n < m. If positive then n > m. Intersection with the S_W = 100% line is $Phi_E \times S_{Wi}$.

Interpretation of Pickett Plots – Effective Porosity and Free Shale Porosity

Pickett plots can be constructed for both the clean formation (Figure 11) and shale (Figure 12). The two porosity/resistivity plots are interpreted to involve quite different values of Archie 'm' and 'n'. For the clean formation (orange data), values are consistent with a standard Archie interpretation of a strongly water-wet system (Figure 11). Alignments of data for S_W < 100% indicate a grouping of data that satisfies the Buckles relation with constants ranging from 0.02 to 0.07.

For the shale formation (Figure 12) a comparison of free shale porosity with resistivity show remarkably different trends. The cementation exponent 'm' is very low (1.14) suggesting linear flow path for low free shale porosity. The saturation exponent 'n' (2.88) suggests an oil-wet system. The interpretation is that free shale porosity is closely associated with organic content, and might indeed be a consequence of porosity creation caused by thermal maturation. As oil is generated, it is the initial fluid injected into the newly-created porosity, which then becomes oil-wet.

Examples

For each example the following plots are presented:

• TOC montage
• Standard density/neutron cross plot
• Shale-only density/neutron cross plot
• Free shale porosity verification plot
• Clean formation total porosity vs. resistivity cross plot
• Free shale porosity vs. resistivity cross plot

Bakken Oil Reservoir, North Dakota (Figure 13, Figure 14, Figure 15)

Niobrara Oil Reservoir, Colorado (Figure 16, Figure 17, Figure 18)

Bakken Oil Reservoir, Montana (Figure 19, Figure 20, Figure 21)

Midland Basin (Wolfcamp) Oil Reservoir, Texas (Figure 22, Figure 23, Figure 24, Figure 25)

Conclusions

A technique is presented to estimate differential reservoir wetting in organic rich reservoir systems using standard open-hole triple-combo logging suites. A minimum combination of GR/density/neutron/resistivity is required. Following a standard shaly formation analysis, data are analyzed to subtract from density and neutron responses the contribution of the non-shale and TOC fractions, level-by-level. For the shale-only porosity log responses, it is then possible to define clay porosity and small volumes of non-TOC shale porosity, here termed Free Shale Porosity.

Two sets of porosity/resistivity cross plots are constructed:

1. Standard total porosity vs. resistivity: This is interpreted to define Archie parameters cementation exponent 'm' and saturation exponent 'n'. From the value of 'n' it is possible to determine reservoir wetting. Low values (mostly less than 2) indicate a water-wet system. In the examples presented here, all are water-wet.

2. Free shale porosity vs. resistivity: All examples show consistently low values of cementation exponent 'm', suggesting linear flow paths for this porosity segment. They also show higher values of the saturation exponent 'n' (sometimes much higher) than for the clean porosity responses, suggesting an oil-wet condition.

It is proposed that the free shale porosity component is generated during the thermal maturation process, as oil is generated and expelled from the organic material. Consequently, the newly generated pore system will be exposed to oil at inception, and is likely to be oil-wet. The very low values of cementation exponent 'm' would suggest that as the porosity system is forming, it is accompanied by the creation of linear flow paths.

References Cited

Archie, G.E., 1942, The electrical resistivity log as an aid to determining some reservoir characteristics: SPE-AIME Transactions, v. 146.

Buckles, R.S., 1965, Correlating and averaging connate water saturation data: Journal of Canadian Petroleum Technology, v. 9/1, p. 42-52.

Glorioso, J.C., and A. Rattia, 2012, Unconventional reservoirs: Basic petrophysical concepts for shale gas: SPE 153004, Vienna, Austria.

Holmes, M., A. Holmes, and D. Holmes, 2009, Relationship Between Porosity and Water Saturation: Methodology to Distinguish Mobile from Capillary Bound Water: AAPG Annual Convention and Exhibition, Denver, Colorado, June 7-10. AAPG Search and Discovery Article #110108 (2009).
http://www.searchanddiscovery.com/documents/2009/110108holmes/ndx_holmes.pdf

Holmes, M., A. Holmes, and D. Holmes, 2014, A New Petrophysical Model to Define Porosity Components of Unconventional Reservoirs, Using Standard Open-hole Triple Combo Logs: SPE Western North American and Rocky Mountain Joint Regional Meeting, Denver, Colorado, April 16-18.

Keller, G.V., 1953, Effect of wettability on the electric resistivity of sand: Oil and Gas Journal, Jan 5.

Passey, Q.R., S. Creaney, J.B. Kulla, F.J. Moretti, and J.D. Stroud, 1990, A practical model for organic richness from porosity and resistivity logs: AAPG Bulletin, v. 74/12, p. 1777-1794.

Pickett, G.R., 1966, A comparison of current techniques for determination of water saturation from logs: SPE 1447, Rocky Mountain SPE, Denver, Colorado, May.

Ransom, R., 1995, Practical Formation Evaluation, John Wiley and Sons, Inc.

Schmoker, J.W., 1989, Use of formation-density logs to determine organic-carbon content in Devonian shales of the Western Appalachian Basin and an additional example based on the Bakken Formation of the Williston Basin: Petroleum Geology of the Black Shales of Eastern North America.

Sweeney, S.A., and H.Y. Jennings, 1960, The electrical resistivity of preferentially water-wet and preferentially oil-wet carbonate rocks, Producers Monthly.
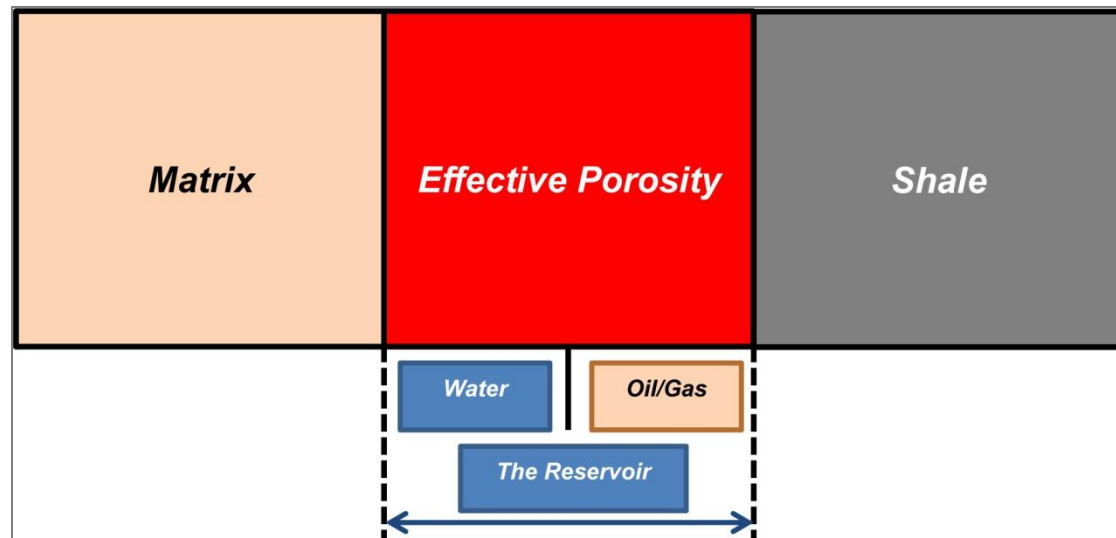
Figure 1. In conventional reservoir analysis, the analysis of shale is to account for excess conductivity due to clay water.
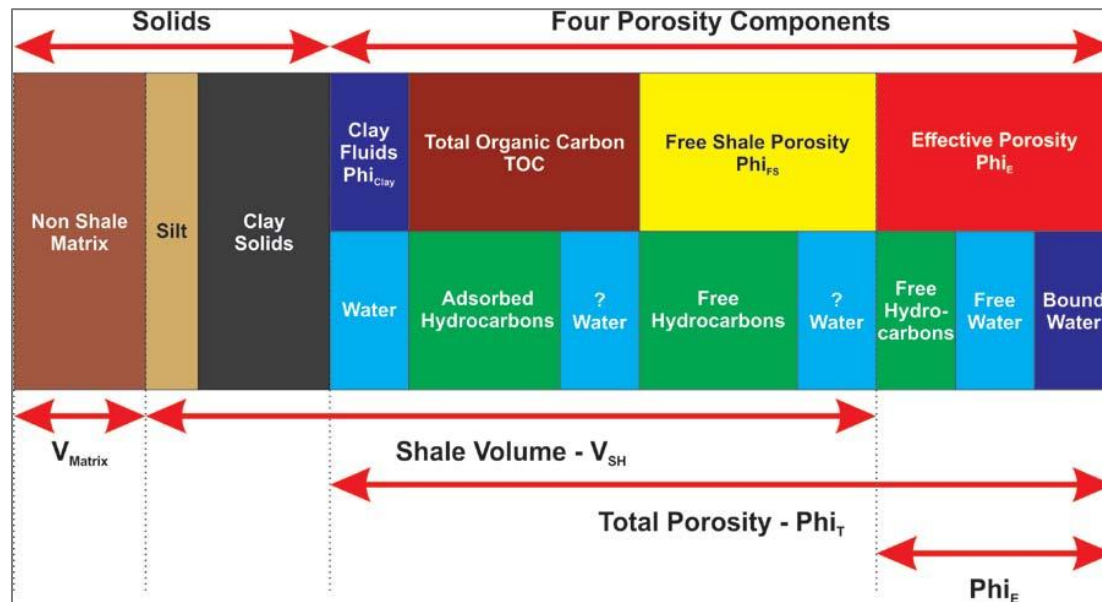
Figure 2. For unconventional reservoirs, properties are quite different from conventional reservoirs, with unique petrophysical attributes. The shale component requires detailed analysis.
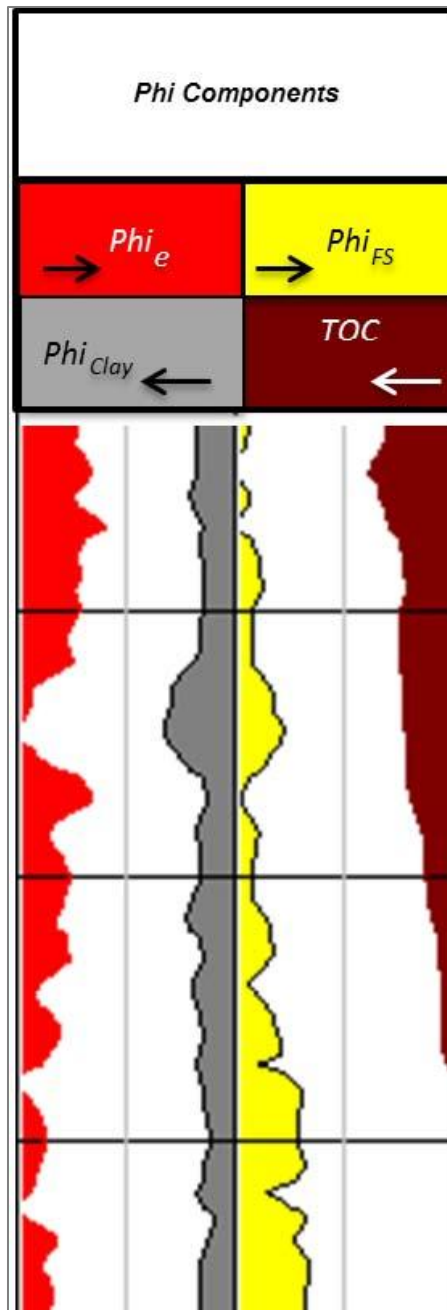
Figure 3. Example depth plot showing the four porosity components.
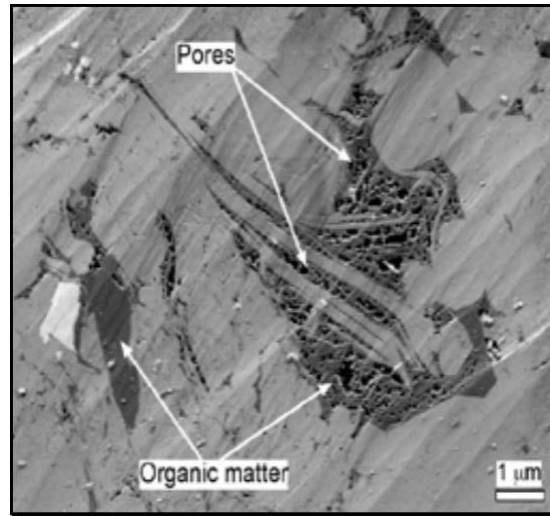
Figure 4. Glorioso - SEM showing pores in organic matter. This can be considered secondary porosity as it results after kerogen maturity and the consequent expulsion of hydrocarbons (Reed, R., BEG 2008).
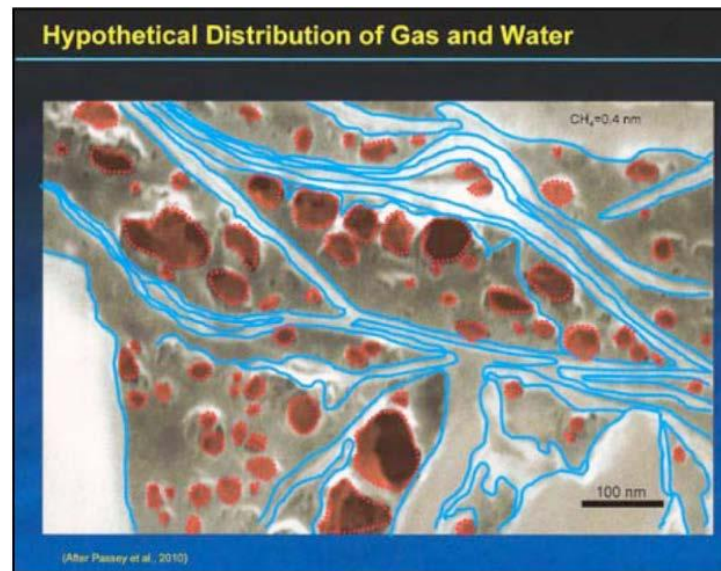
Figure 5. Fluid distribution in the porous system according to Passey; free gas (dark red) in kerogen pores, adsorbed gas in the kerogen pore wall (light red) and water (light blue) in the inorganic matrix that looks microfractured (Passey, 2010).
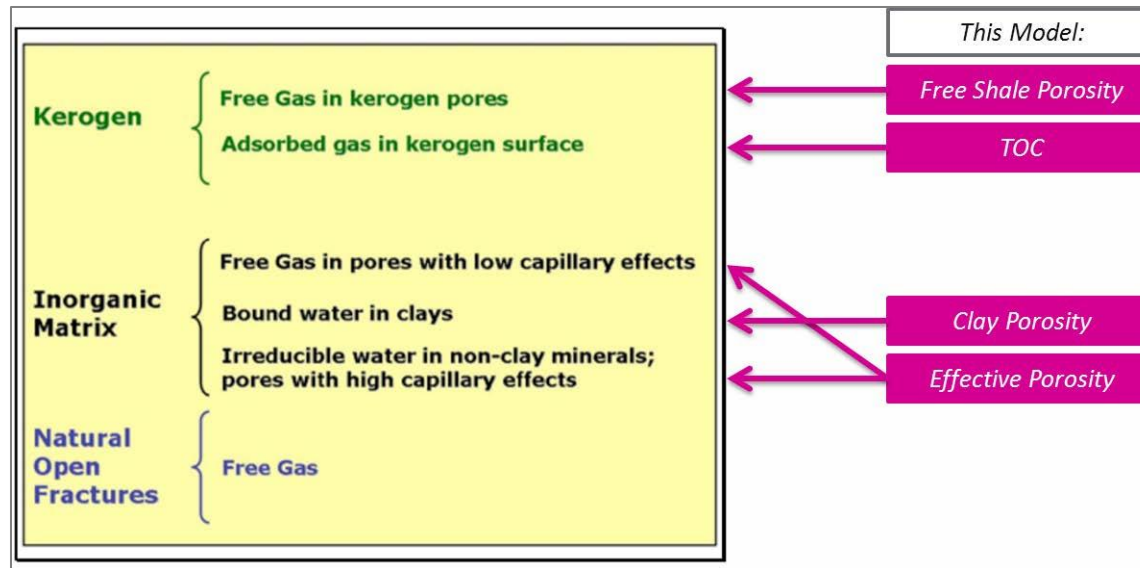
Figure 6. Fluid distribution in porous shale; includes natural fractures.
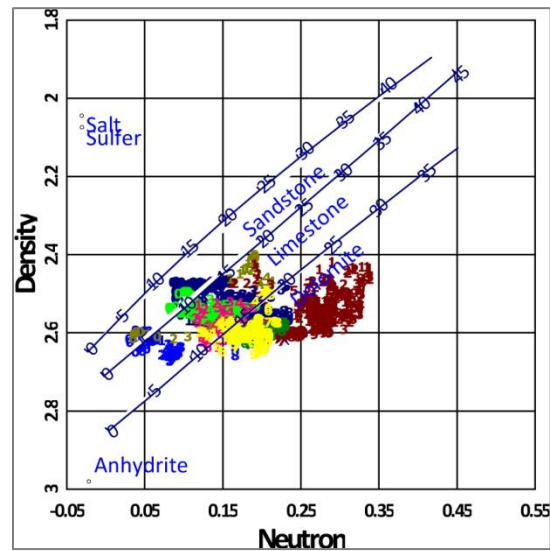
Figure 7. Density/neutron cross plot porosity.
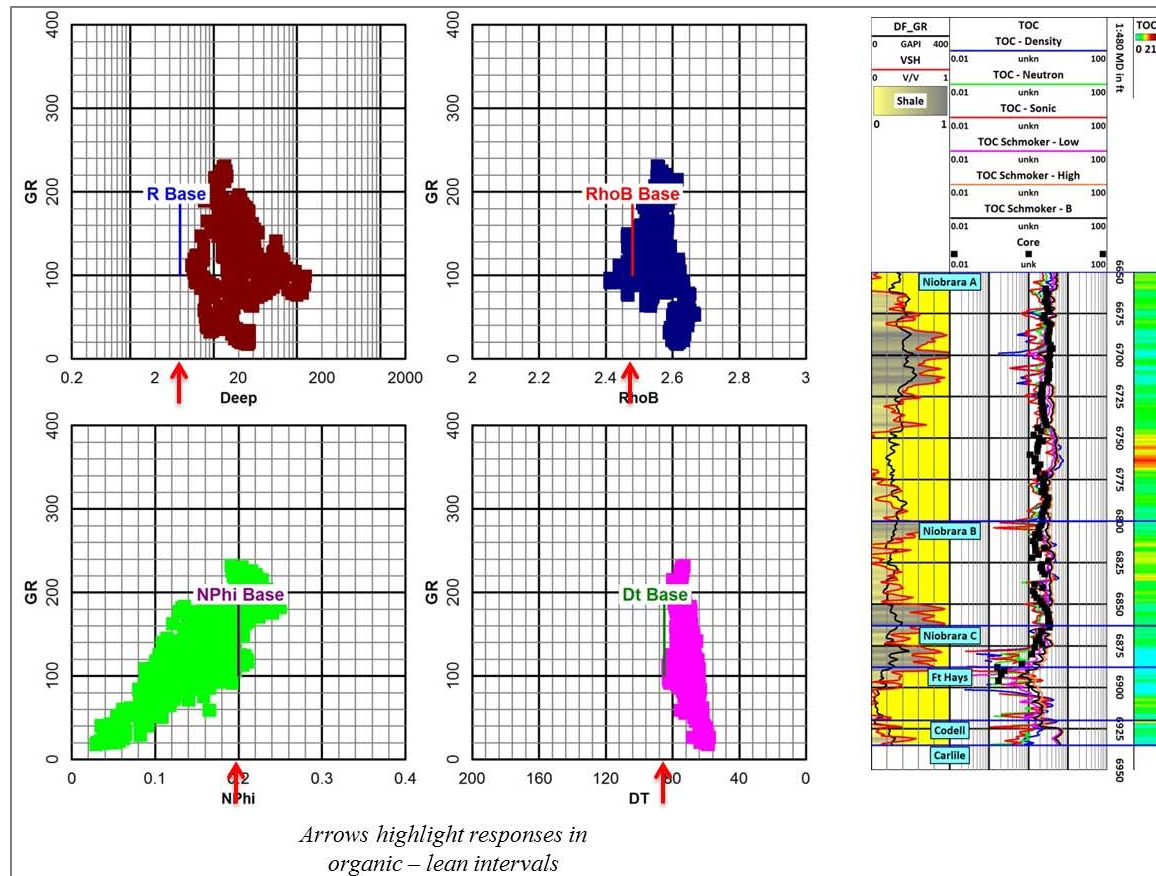
Figure 8. Passey – calibrating for ΔlogR (left) and the output (right) for TOC from the Passey and Schmoker techniques.
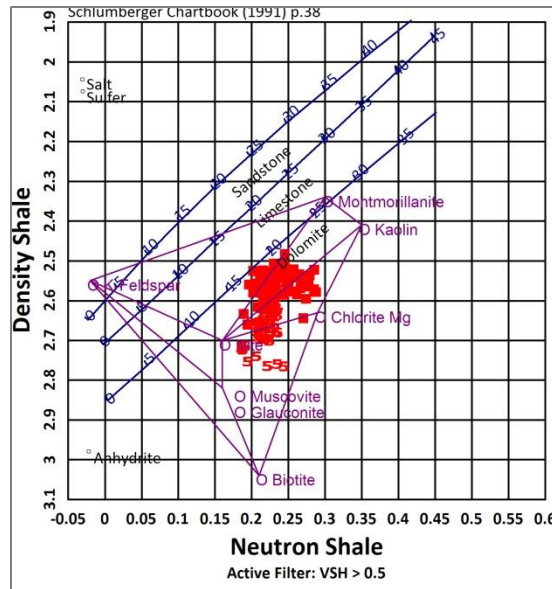
Figure 9. Shale-only density/neutron comparison.
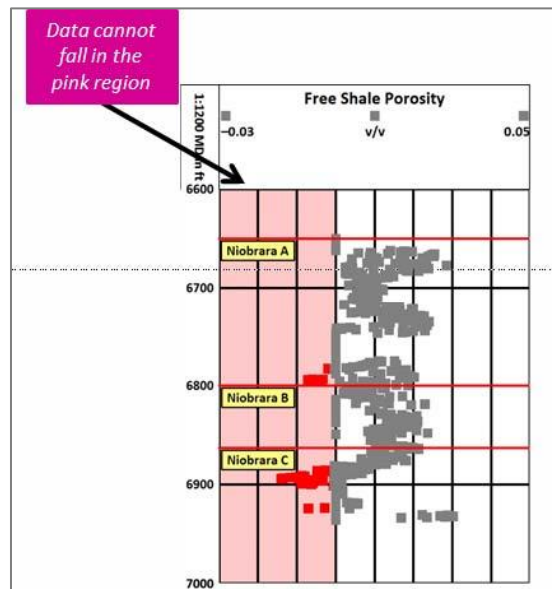
Figure 10. Depth plot of Free Shale Porosity - negative values are impossible and indicate the need to revisit the Free Shale Porosity calculations.

R_W

aRw 80 60 40 20

Total Porosity

Orange: $V_{SH} < 30\%$
Grey: V_{SH} 30-75%
Black: $V_{SH} > 75\%$

Measure of
$m - n$

PhiSwi

Data trend:
$Phi \times S_{Wi} = constant$

10%

Strongly water-wet
in effective porosity

S_W

Slope $= {-1}/{m}$

100%

Rw =   0.014
Archie's 'a' =   1
Archie's 'm' = 1.8
Archie's 'n' = 1.6
Phi Swi =   0.03

$$S_W{}^n = \frac{R_W}{Phi^m R_t}$$

Rt (ohm meters)
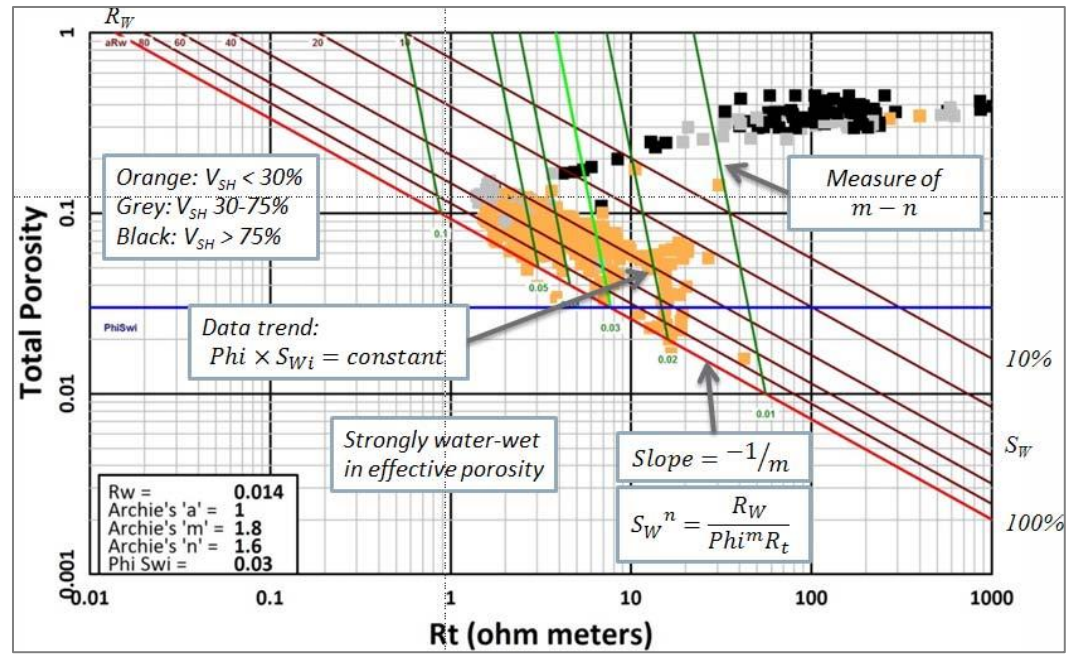
Figure 11. Clean formation Pickett Plot using Total Porosity.
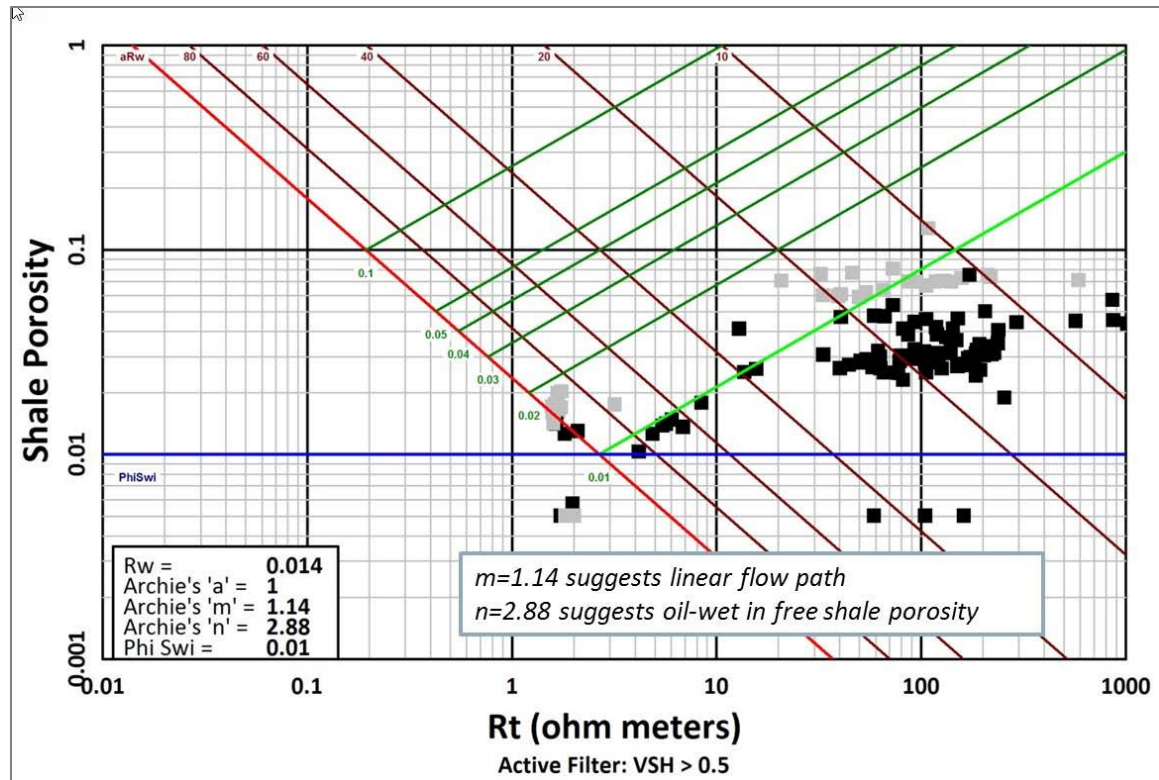
Figure 12. Shale fraction Pickett Plot using Free Shale Porosity. The data suggests an oil-wet system for the Free Shale Porosity fraction.
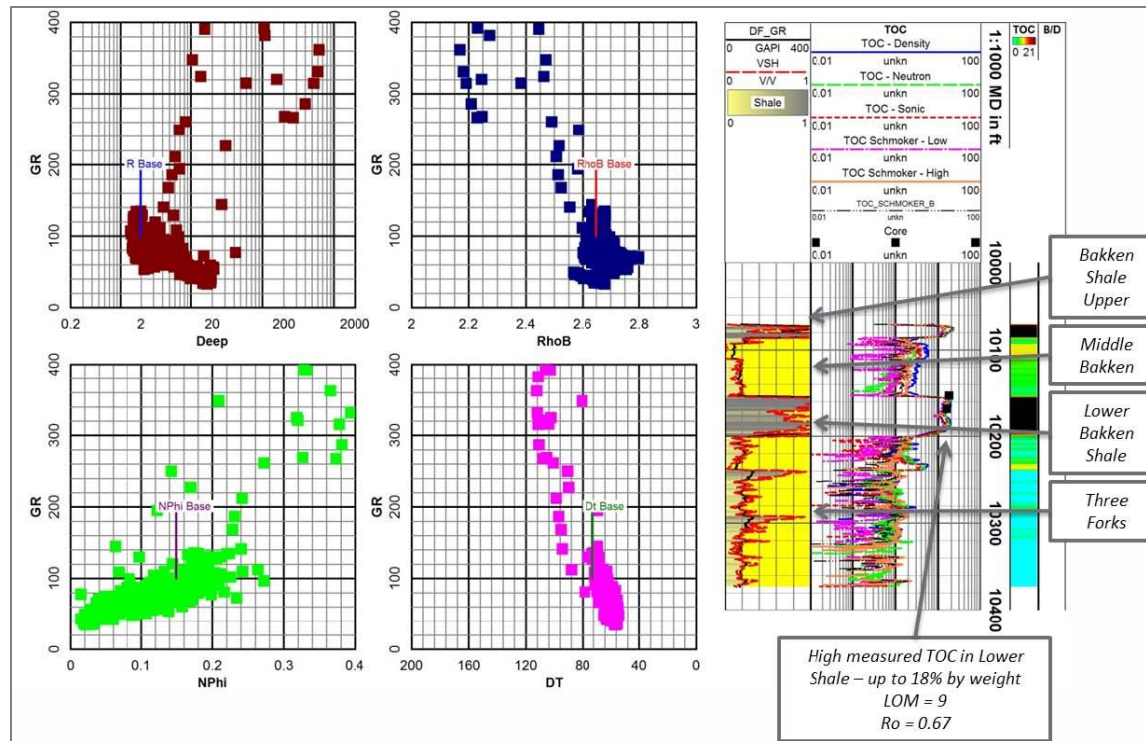
Figure 13. Bakken oil reservoir – TOC montage.
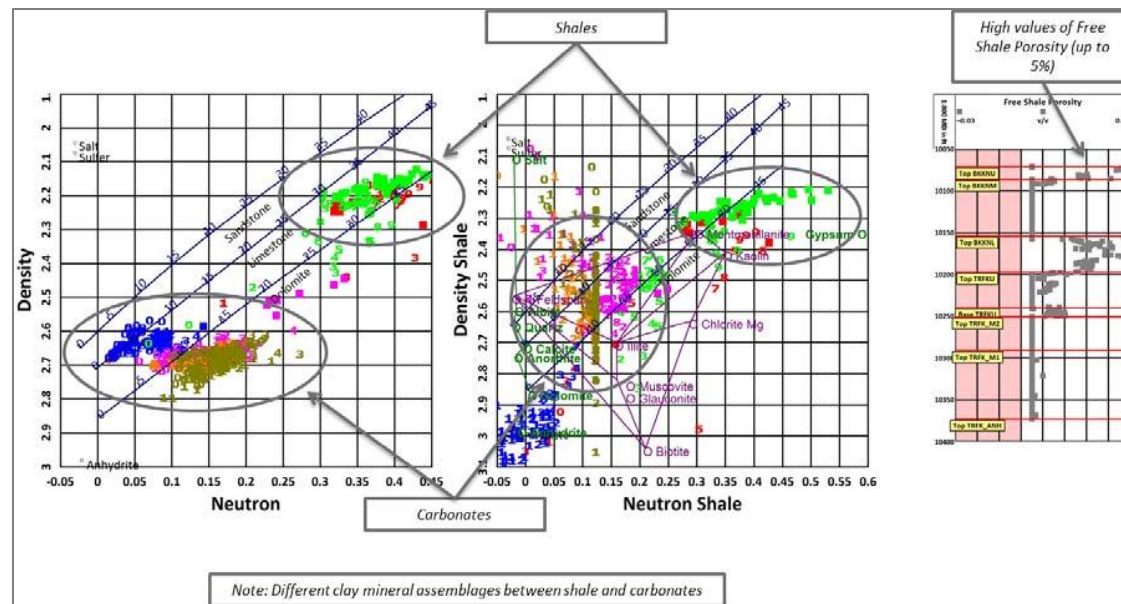
Figure 14. Bakken oil reservoir – clean and shale density/neutron cross plots and free shale porosity verification plot.
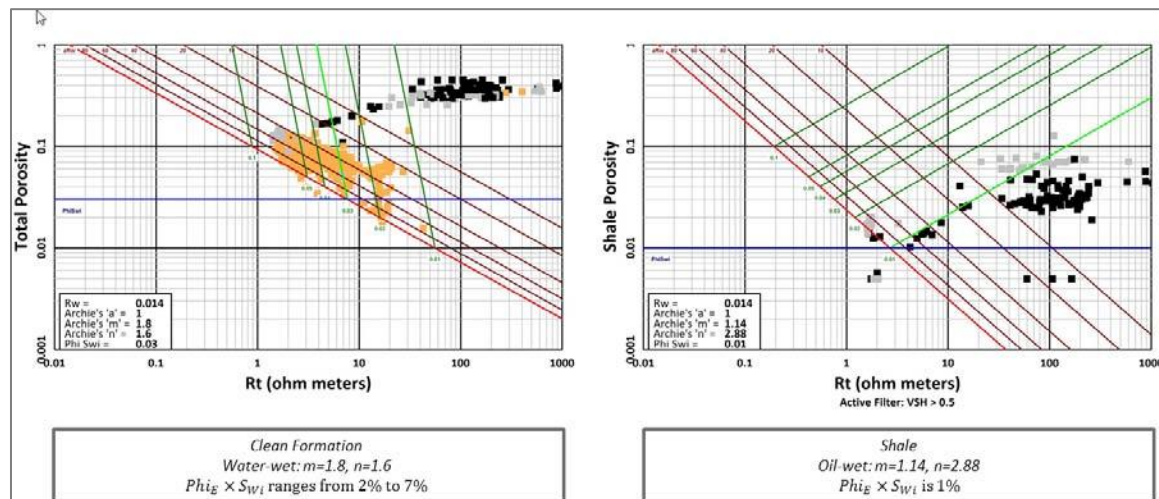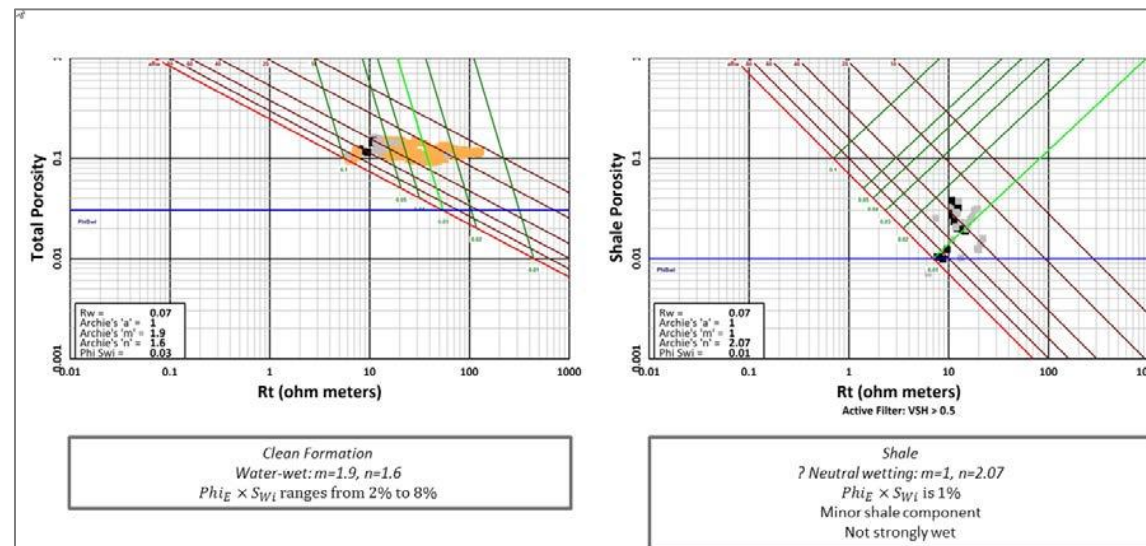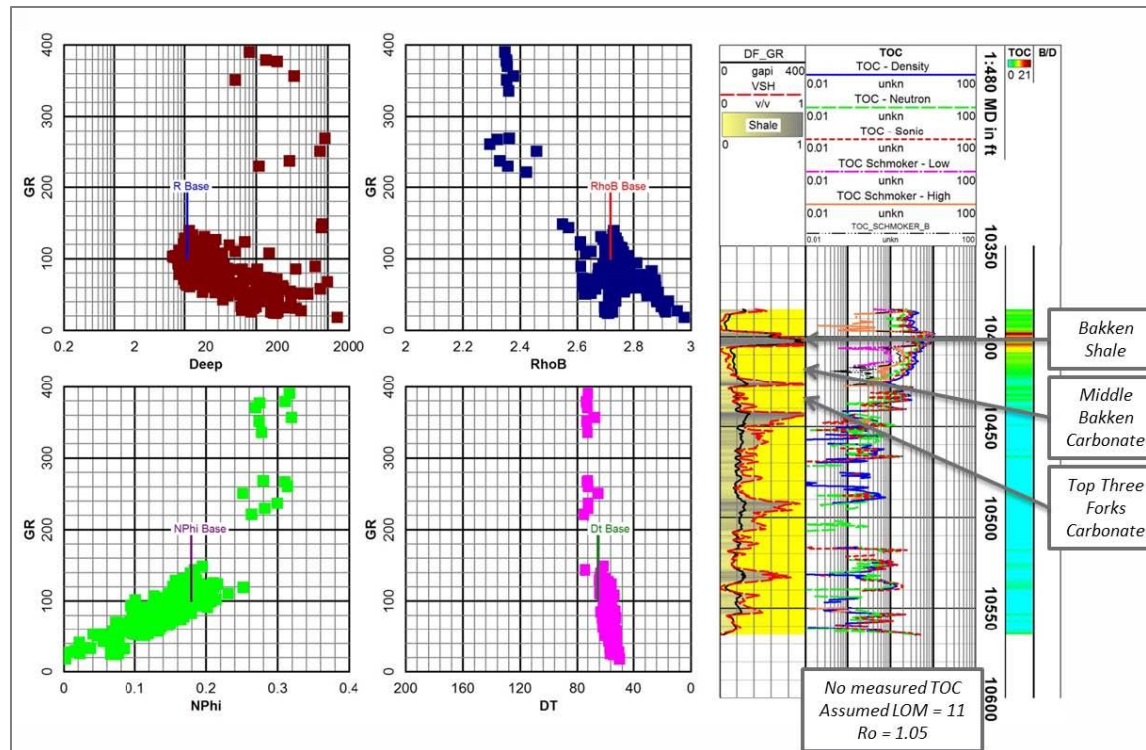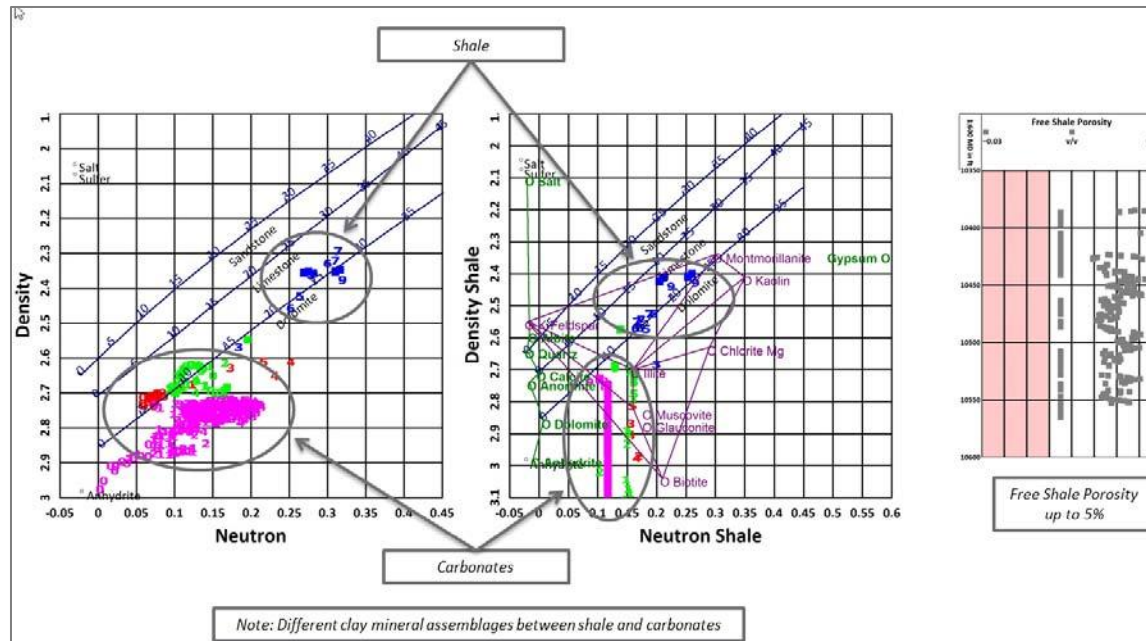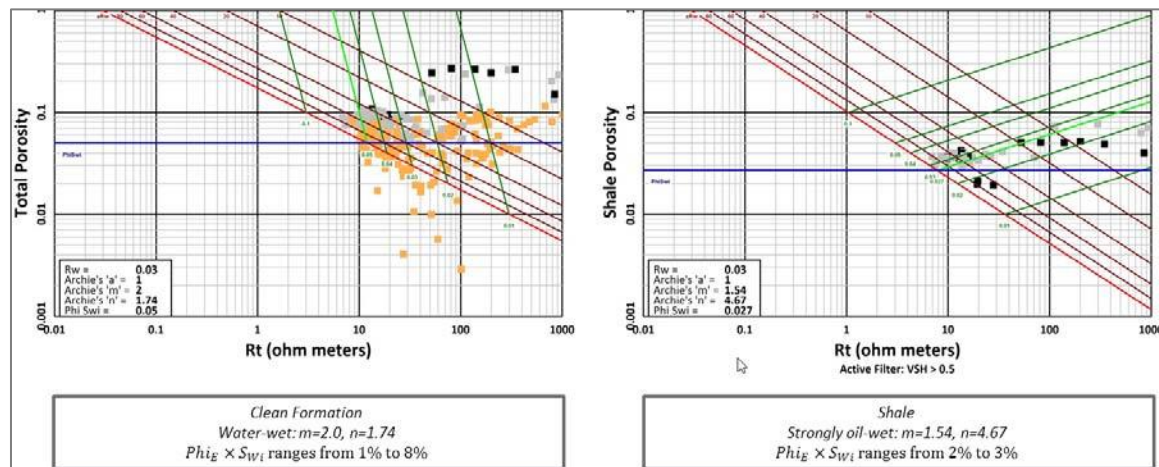

Figure 15. Bakken oil reservoir – clean and shale Pickett plots.
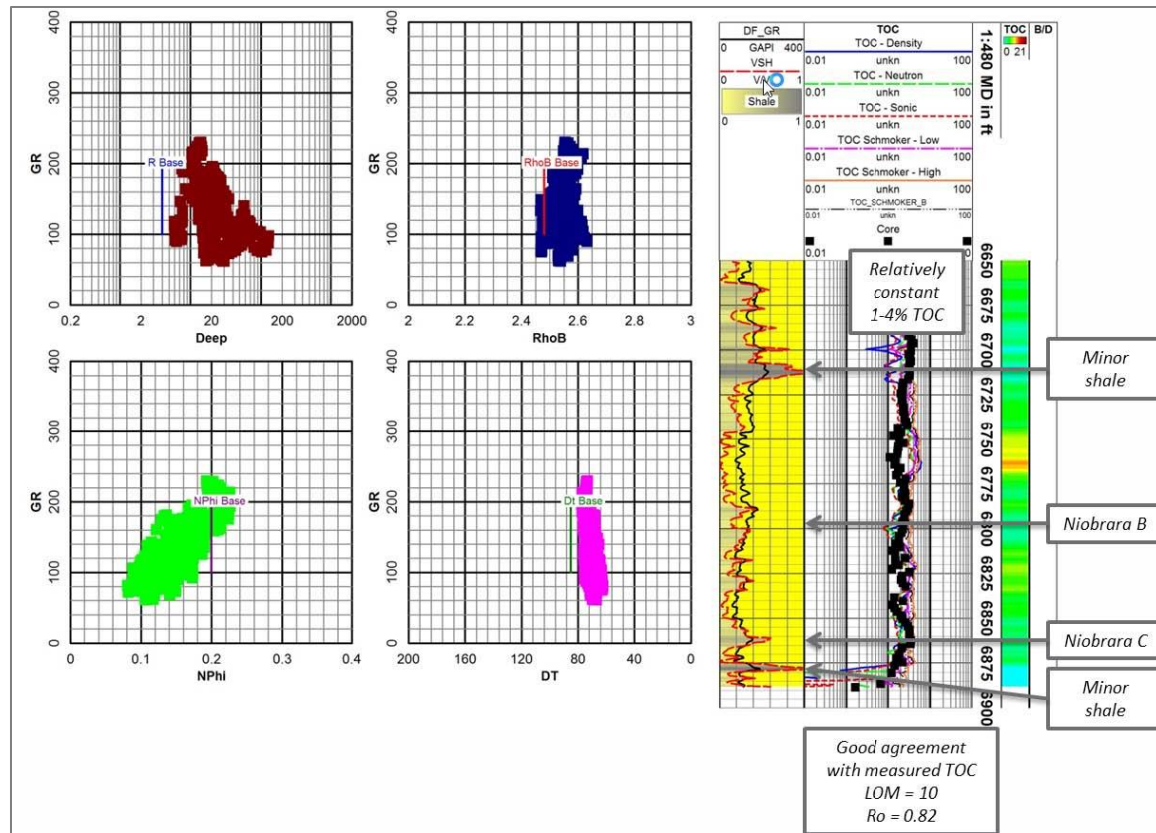
Figure 16. Niobrara oil reservoir – TOC montage.
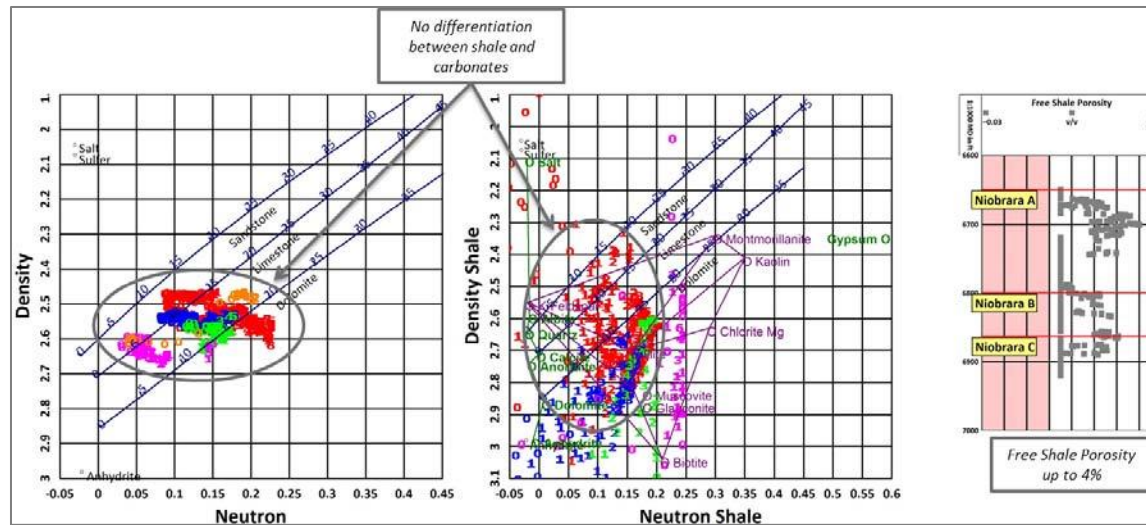
Figure 17. Niobrara oil reservoir – clean and shale density/neutron cross plots and free shale porosity verification plot.

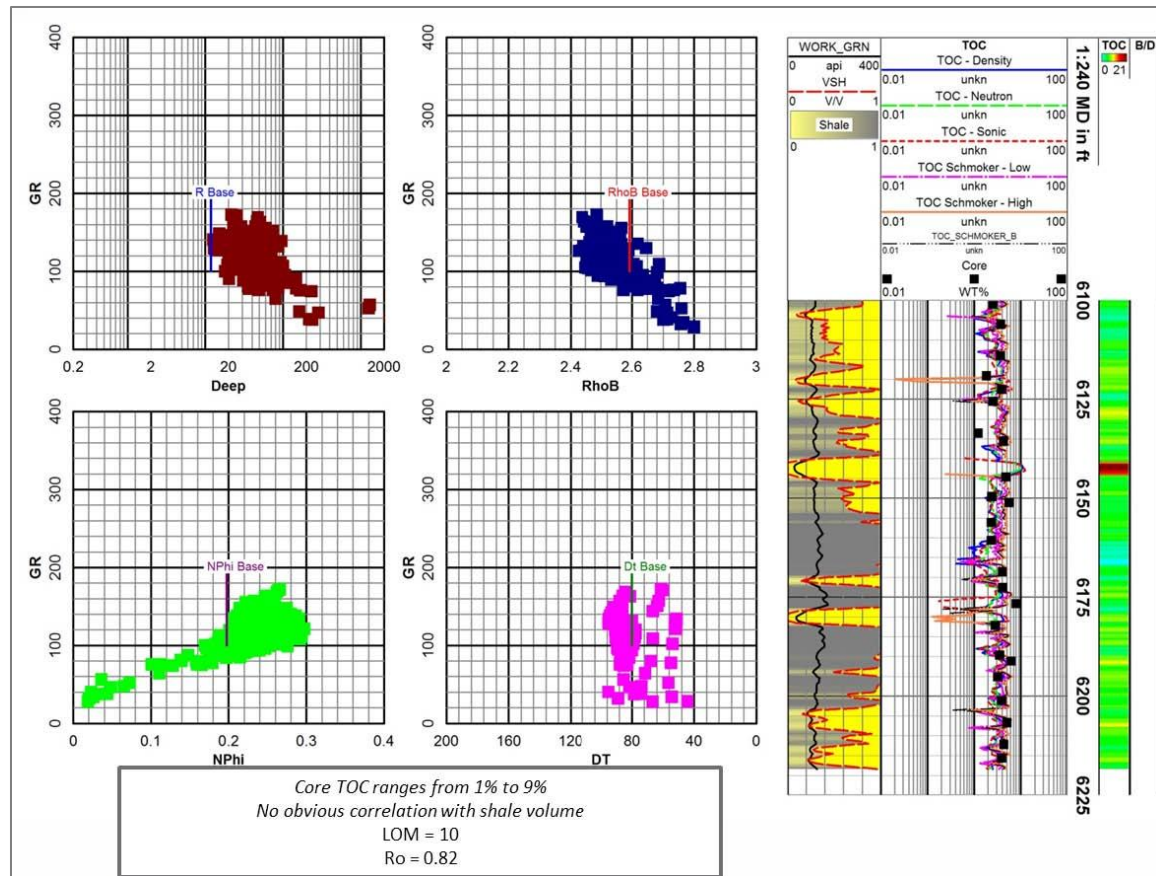Figure 18. Niobrara oil reservoir – clean and shale Pickett plots.

Figure 19. Bakken oil reservoir – TOC montage.

Figure 20. Bakken oil reservoir – clean and shale density/neutron cross plots and free shale porosity verification plot.

Figure 21. Bakken oil reservoir – clean and shale Pickett plots.

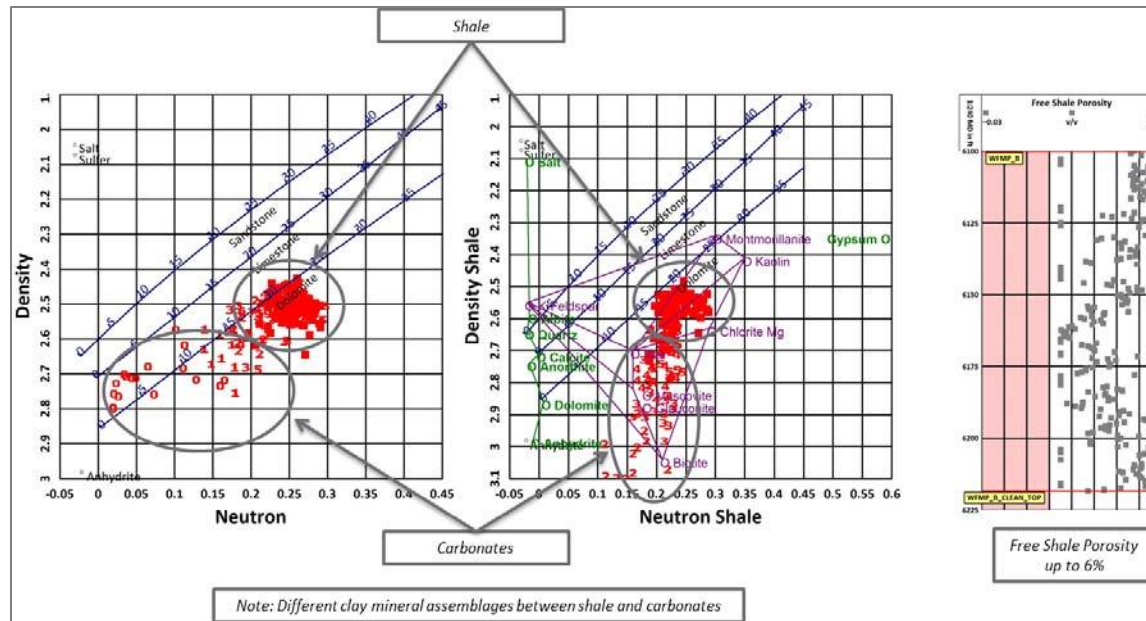Figure 22. Midland Basin (Wolfcamp) oil reservoir – TOC montage.

Figure 23. Midland Basin (Wolfcamp) oil reservoir – clean and shale density/neutron cross plots and free shale porosity verification plot.
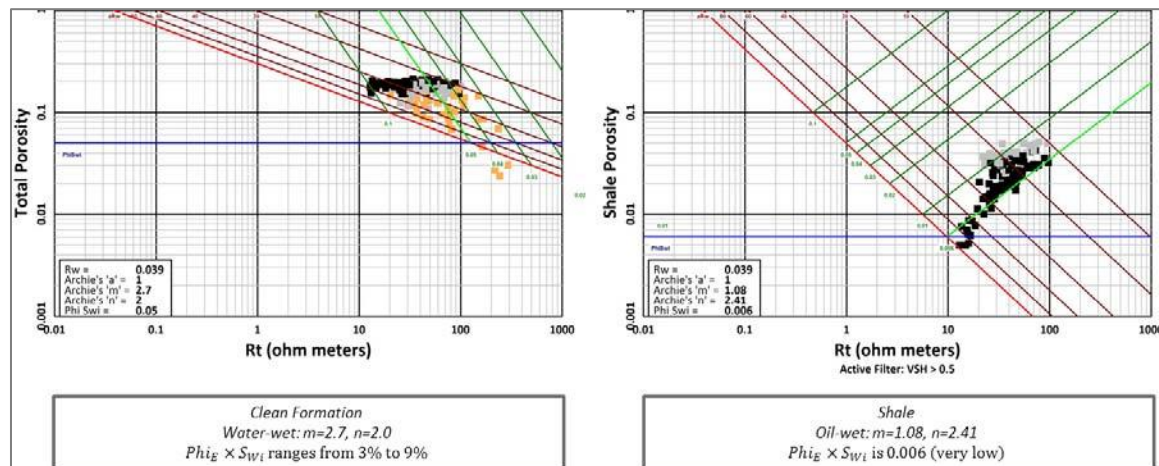

Figure 24. Midland Basin (Wolfcamp) oil reservoir – clean and shale Pickett plots.

Figure 25. Midland Basin (Spraberry) oil reservoir – TOC montage.
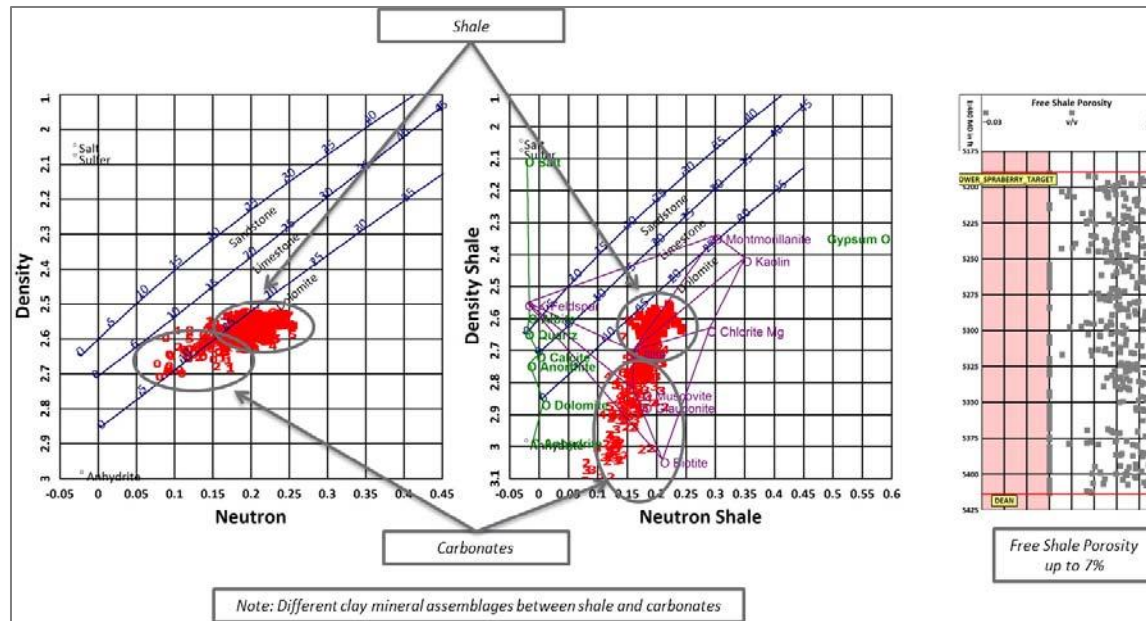
Figure 26. Midland Basin (Spraberry) oil reservoir – clean and shale density/neutron cross plots and free shale porosity verification plot.
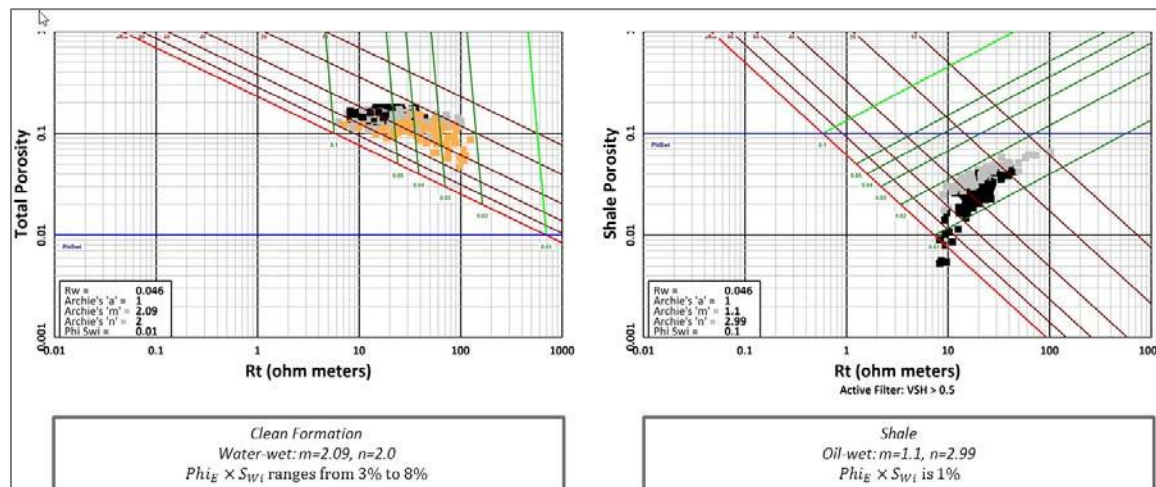

Figure 27. Midland Basin (Spraberry) oil reservoir – clean and shale Pickett plots.